Auto-coherent homogenization applied to the assessment of thermal conductivity: Case of sugar cane bagasse fibers and moisture content effect

Cristel Onesippe Potiron, Ketty Bilba, Atika Zaknoune, Marie-Ange Arsène

Auto-coherent homogenization applied to the assessment of thermal conductivity: case of sugar cane bagasse fibers and moisture content effect

Cristel Onésippe Potiron[1*], Ketty Bilba[1], Atika Zaknoune[1] and Marie-Ange Arsène[1]

[1] Université des antilles - Laboratoire COVACHIM-M2E EA 3592, UFR SEN, Campus de Fouillole. BP 250 97157 Pointe-à-Pitre, Guadeloupe, France (FWI).

*corresponding author : cristel.onesippe@univ-antilles.fr

ketty.bilba@univ-antilles.fr, atika.zaknoune@univ-antilles.fr, marie-ange.arsene@univ-antilles.fr

*Phone : +590 (590) 483217

Abstract

The purpose of this study is to evaluate the thermal conductivity of sugar cane bagasse fibers when they reinforce vegetable fibers/cement composites using auto-coherent homogenization. The moisture content effect on the thermal conductivity of composites is also studied. When the fiber content increases, porosity increases according to a linear rule and bulk density and thermal conductivity of composites decrease. When the moisture content grows, the thermal conductivity of composites increases. When applying auto-coherent homogenization, in dry state, results show a gap of less than 10% between experimental and modeled values of composites thermal conductivity and a mean sugar cane bagasse fibers thermal conductivity of 0.110 W/m.K. In wet state (56% RH), there is an approximate agreement of 1,4% between estimated and experimental values of thermal conductivity of composites up to 4 wt% of fibers content.

Keywords : Natural fibers ; Thermal properties ; Cement composites ; Auto – coherent homogenization; Moisture content.

1. Introduction

Guadeloupe (French West Indies) is a Caribbean island with a tropical climate [1, 2] were various vegetable fibers, including agro – industrial wastes, are low-cost and/or abundantly available [3-4]. This archipelago has a high seismicity and is prone to violent hurricanes [5]. Therefore, the main construction material used in the building sector is conventional cement and its derivatives (concrete blocks, bricks, …) [6-7].

French thermal and acoustic regulations advocate the use of 50% renewable power in energy consumption by 2020 [7]. One way to reduce the energy consumption, as consequence to increase the renewable energy ratio, is to use less air-conditioning in infrastructures [7]. To achieve this goal, the partial replacement of cement by vegetable fibers as reinforcement of cementitious matrix is considered [1, 3, 6, 7]. Indeed, vegetable fibers are known to have insulating properties that is to say a low thermal conductivity and appear to be a good alternative to synthetic fibers such as glass fibers or asbestos fibers, commonly used for building insulation [8-10]. As observed by Onésippe et al. in 2010 [3] and even now, few works have demonstrated the low thermal conductivity of vegetable fibers cement-based composites as well as the thermal

conductivity of vegetable fibers (when they are incorporated in the composites) and the influence of moisture on thermal conductivity of these composites. The presence of wood fibers reduces the density of the material [11] and decreases its thermal conductivity [3, 6, 10].

Vegetable fibers are vulnerable to alkalinity of matrix thus causing debonding of the fiber / matrix interface and thus a decrease in the mechanical performance of the composites [3, 9]. To limit vulnerability of vegetable fibers in the matrix, various treatments of fibers have been considered such as chemical (acid or alkaline), physical-chemical, thermal and mechanical treatments [9, 11]. These various treatments lead to a strengthening of fiber/matrix interface [12] because they induce, on the one hand, the modification of the morphology of the fibers and, on the other hand, the reduction of the contents of hemicellulose and extractible materials which are inhibitors of the hydration of the binder [12].

Moreover, vegetable fibers are hydrophilic and their high affinity for water may thwart the hydration of matrix [13]. To overcome this competition, some authors propose the pyrolysis [12, 14] or the pre-wetting [15-18] of vegetable particles to retain their original volume (porosity) and so, play a role of water tank during the setting phase of the binder. Collet [13] recommends a pre-wetting of the binder with water prior to its addition to vegetable particles in order to ensure a good hydration of binder and to avoid competition between cement and fibers hydration [19].

The purposes of this study are to (1) estimate the modeled value of thermal conductivity of vegetable fibers when they reinforce cement matrix and (2) measure the effect of moisture content on vegetable fibers/cement composites thermal properties. To reach these goals, cement composites reinforced by various amounts of sugar cane bagasse fibers ranging from 2 to 8 wt % were considered. Sugar cane bagasse fibers are widely available in Guadeloupe : according to Food Directorate of Agriculture and Forestry from Guadeloupe, the island produces 680000 tons/year of sugar cane mainly used for the sugar and rum industries [20]. Bagasse is the solid lignocellulosic leftover after extraction of juice from the sugar cane stalk and is cheap compared to synthetic fibers [21].

In order to achieve the modeling of thermal conductivity of fibers, the first part is dedicated to the study of bagasse fibers / cement composites : measurements of thermal conductivity and physical-chemical characteristics (density, apparent volume and porosity). The thermal conductivity is studied at three different moisture contents. In the second part, a model of thermal conductivity of fibers and composites, in dry and wet states, is applied. The purposes of this work is (1) to propose a way to assess the thermal conductivity of bagasse fibers incorporated in this kind of composites, as very few data's of thermal conductivity of vegetable fibers are available and (2) to compare the (experimental and numerical) behaviors of composites when they are placed in different relative humidity (RH) to establish, if possible, a relation between thermal conductivity of composites and RH. Generally, in the literature, many models make it possible to estimate the thermal conductivity of dry concrete and dry composite materials on the basis of knowing the conductivity of each component and its concentration [22-27]. Several of them are based on the auto-coherent homogenization (HAC) model [25-28]. This model uses the statements of self-consistent field concept and of spherical geometry of inclusions in composites; for examples:

- autoclaved aerated concrete for Boutin [29],

- synthetic foams in continuous medium for Felske [30],
- wood shaving and concrete for Bederina et al. [25],
- cement composites containing rubber waste particles by Benazzouk et al. [26],
- hemp concretes by Collet and Pretot [28] ,
- insulating building materials made from date palm fibers mesh by Boukhattem et al. [26].

Among them, Felske [30], established equations allowing the estimation of the thermal conductivity of regular hollow spheres particles (synthetic foam), while the other previous authors [25-29] focused on a distribution of spherical particles with different diameter. Although the geometries involved are the same as in our materials, it appears that Felske's special case and critical values are not suitable in this study because Felske assumed that the particles are uniform. Bagasse fibers, being vegetable matter, are not uniform [31] and more, there is no perfect thermal contact between the vegetable matter and the cementitious matrix. Finally, the auto-coherent homogenization equations, as described by [25-29], were chosen because they are well suited to materials with very different pores sizes (such as concrete) [29] and they are currently employed when studying thermal conductivity of concrete.
Thus, in this work on vegetable fibers/cement composite materials,

- a focus has been made on the model already confirmed and largely used in the field of cementitious materials containing vegetable matter that is to say the HAC model,
- this HAC model as described by [22-29] has been applied to assess the numerical value of thermal conductivity of bagasse fibers/cement composites in wet and dry states and it was possible for us to deduce the thermal conductivity of sugar cane bagasse fibers in the cement composites.

To our knowledge, very few models of thermal conductivity of vegetable fibers / cement composites and even less models of the thermal conductivity of vegetable fibers alone are proposed in the literature [3, 8].

2. Materials

2.1 Sugar cane bagasse fibers

Sugar cane bagasse fibers are named NBF and were collected from Montebello distillery (Petit-Bourg, Guadeloupe, FWI). Fibers were crushed with a knife mill (Restch, France) and sieved in the laboratory to obtain final length varying from 1 to 10 mm and width between 0.4 and 1 mm. The sugar cane bagasse fibers chemical composition has already been determined [32] and is summarized in Table 1.

2.2 Binder

The binder was a white Portland cement CEM I 52.5 N manufactured by Axton society. This Portland cement CEM I 52.5N complies with European standard EN 197-1 [33]. Its chemical composition and some of its physical characteristics are presented in Table 2.

2.3 Composites formulations and preparation

A reference sample (i.e. without any fibers) has been prepared. It is named L. Composites were made by mixing each type of binder with various amounts of sugar cane bagasse fibers. Formulations of composites, named LFN, are presented in Table 3. All composites were prepared according to the mixing sequence indicated in Table 4 and tap water was used.

The obtained pastes were casted in normalized molds of dimensions 40*40*160 mm^3. According to EN 196-1 standard [34], a compaction (10 strokes by step – 2 steps) with a shaking table was applied to each sample. Then the isotropic samples, with a random repartition of fibers in the binder, were removed from the mold and left for curing during 28 days in a climatic chamber (25°C, RH = 70%).

3. Methods

3.1 Bulk dry density, apparent volume and porosity measurements of composites

The bulk dry density ρ_A was deduced from the dry mass and apparent volume of samples. To determine the dry mass, samples were placed in an oven at 105°C (+/- 1°C). The dry state was reached once the mass of each sample was stabilized.

The apparent volume of each sample was measured by using a sliding caliper (accuracy of +/- 0.01 mm). Each mean dimension is calculated from an average of three measurements.

Composites true density ρ_V has been measured using helium gas intrusion under helium gas flow with a "Pycnomatic" Thermo Electron Corporation equipment (France) pycnometer. Five measurements were conducted for each composite at 298 K, relative humidity of 70–80%. The open porosity η is deduced from bulk dry and true densities using equation (1):

$$\eta = 1 - \frac{\rho_A}{\rho_V} \qquad \text{equation 1}$$

where ρ_A is bulk dry density, ρ_V is true density of samples and η is open porosity.

3.2 Thermal conductivity testing

The tests were performed with a C-therm TCi unit (Setaram, France). The C-Therm TCi employs the Modified Transient Plane Source (MTPS) technique. The one-sided, interfacial heat reflectance sensor applies a momentary constant heat source to the sample. A known current is applied to the sensor's spiral heating element, providing a small amount of heat. The sensor's guard ring is fired simultaneously supporting a one-dimensional heat exchange between the primary sensor coil and the sample. The current applied to the coil results in a rise in temperature at the interface between the sensor and sample, which induces a change in the voltage drop of the sensor element. The increase in temperature is monitored with the sensor's voltage and is used to determine the thermo-physical properties of the sample. The thermal conductivity is inversely proportional to the rate of increase in the sensor voltage (or temperature increase). Thermal conductivity is measured directly [35].

For precise measurement of thermal conductivity, samples are first polished using a rotate polishing machine with sandpaper (Dremel, USA). Three levels of moisture are evaluated: 0%, 56% and saturated state 100% of relative humidity. We choose 56% RH as an intermediate value in relative humidity because, in real conditions, cement composites do not reach dry-oven or saturated conditions. The dry state (0% RH) is obtained by drying the material in an oven at 105°C (+/- 1°C) and then placing it in a

desiccator until the time of testing. To measure the thermal conductivity at 56 % RH, samples are placed in a desiccator whose humidity is controlled using saturated saline solutions of sodium bicarbonate. Local measurements are made on the lateral and transverse sides of samples and an average value is calculated. To ensure that the moisture content has not changed, samples are weighed before and after measurement.

3.3 Modeling of thermal conductivity of composites by auto-coherent homogenization

The auto-coherent homogenization is used in order to model the thermal conductivity of bagasse fibers / cement composites. This method was initially developed for the mechanical characterization of composites materials [25-26] and was then extended to electrostatic, magnetostatic, electric conduction and thermal properties, which are mathematically analogous [18, 28]. The principle of the method is that the heterogeneous material is assimilated to an equivalent homogeneous material, which must be characterized (knowledge of the conductivity of each component and its concentration). Thus, a transition of micro-scale (components) to macroscopic scale (material) allows to express overall thermal conductivity in terms of characteristics of each component (conductivity, volume concentration).

3.3.1 Dry state

The auto-coherent homogenization is well described by Collet and Pretot [28]. Briefly, the dried material is considered as an assembly of spherical inclusions of various sizes. In the case of material with two-components, it is meant to be a sphere of radius R_a and thermal conductivity λ_a (component "a" is the air contained within the vegetable fibers) surrounded by a concentric shell of component "s" (s is the fiber block) of thermal conductivity λ_s and radius R_s. λ_d is the thermal conductivity of the equivalent homogeneous material also called effective conductivity (Figure 1).

The expression of effective conductivity λ_d (equation 2) is obtained by assuming that the energy contained in the heterogeneous medium is equivalent to that of the homogeneous medium under the same boundary conditions [26, 28].

$$\lambda_d = \lambda_s = \left[1 + \frac{\varepsilon}{\frac{1-\varepsilon}{3} + \frac{1}{\lambda_a/\lambda_s - 1}} \right]; \quad \varepsilon = \left(\frac{R_a}{R_s} \right)^3 \qquad \text{equation 2}$$

where ε is the volume concentration of air phase: it is assumed that the concentration of unconnected phase is equal to the ratio of external and internal pores [29].
According to Boutin [29], this assumption is only satisfied if the material consists of an assembly of composites spheres of variable sizes. Collet and Pretot [28] made this same assumption in case of hemp concrete composites, which are close to bagasse cementitious composites of this study.

We assume that the fibers / dry binder composite is a three components material. In that case, the tri-composite inclusion method is used for the modeling of thermal conductivity assuming that a spherical air bubble "a" is surrounded by a concentric vegetable particles shell "f " itself surrounded by a binder shell "s" (Figure 2).

This type of wildcard inclusion is based on three assumptions:

- the binder consists of cement and microscopic air bubbles trapped in closed-pores;
- the vegetable particles consist of plant part and intra-particle air;
- the air bubble is the microscopic and macroscopic air contained in open pores of material.

The expression of thermal conductivity of vegetable fibers / cement composites is therefore given by equation 3.

$$\lambda = \lambda_s \left[1 + \frac{\theta}{\frac{1-\theta}{3} + \frac{1 + \frac{\delta}{3}\left(\frac{\lambda_a}{\lambda_f} - 1\right)}{\frac{\lambda_a}{\lambda_s} - 1 - \frac{\delta}{3}\left(\frac{\lambda_a}{\lambda_f} - 1\right)\left(\frac{2\,\lambda_f}{\lambda_s} + 1\right)}} \right] \qquad \text{equation 3}$$

where $\theta = 1 - \frac{1}{k+1}\left(\frac{\rho}{\rho_s}\right)$, $\delta = \frac{\rho}{\rho_f}\,\frac{k}{k+1}\,\frac{1}{1 - \frac{\rho}{\rho_s}\frac{1}{k+1}}$ and $k = m_f / m_s$

θ and δ are concentrations directly calculated from the mass m of each component (of known density ρ). This definition of k is based on the assumption that the change of properties between powdered cement and dry hydrated cement (i.e. hydrated cement at 0%RH) does not cause a significant variation in the thermal conductivity of composite [15]. For each formulation, the characteristic parameter k is calculated as the ratio between the mass of bagasse fibers and the mass of powdered cement [25].

3.3.2 Wet state

The modeling process of wet composite involves two steps:

- the first step allows creating homogeneous medium "sf" of vegetable particles "f" and hydrated binder "s" at 0% RH,
- in the second step, the homogeneous medium "sf" is included in a tri-composite (air, water, "sf") model to obtain the final homogenized wet composite. The vegetable fibers "f" and dry binder "s" are therefore considered as a homogeneous medium "sf" and not as two separated phases (Figure 3).

Equation 4 gives the expression of equivalent conductivity of "sf" composite as a function of conductivity of each component (fibers and hydrated binder at 0% RH). The parameter ε' is used to evaluate the volume concentration of fibers in the binder.

$$\lambda_{sf} = \lambda_s \left[1 + \frac{\varepsilon'}{\frac{1-\varepsilon'}{3} + \frac{1}{\lambda_f/\lambda_s - 1}} \right] \quad ; \quad \varepsilon' = \left(R_f/R_s\right)^3 = \frac{1}{1 + k\frac{\rho_f}{\rho_s}} \qquad \text{equation 4}$$

where λ is for the thermal conductivity, k is the ratio of mass (as defined in equation 3) and ρ is the density.

In the second step, the tri-composite inclusions model allows expressing the conductivity of composite in wet states (equation 5).

$$\lambda_H = \lambda_{sf} \left[1 + \frac{\theta}{\frac{1-\theta}{3} + \frac{1 + \frac{\delta}{3}\left(\frac{\lambda_a}{\lambda_w} - 1\right)}{\frac{\lambda_a}{\lambda_w} - 1 - \frac{\delta}{3}\left(\frac{\lambda_a}{\lambda_w} - 1\right)\left(2\frac{\lambda_w}{\lambda_{sf}} + 1\right)}} \right] \qquad \text{equation 5}$$

$$k_1 = \frac{m_w}{m_s + m_f}, \quad \theta = \left(\frac{R_w}{R_{sf}}\right)^3 = 1 - \frac{1}{1 + k_1}\frac{\rho_h}{\rho_{sf}} \text{ and } \delta = k_1 \frac{\rho_{sf}}{\rho_w}\left(\frac{1}{1 - \frac{\rho_H}{\rho_{sf}}\frac{1}{k_1 + 1}} - 1\right)$$

λ is for the thermal conductivity, k is the ratio of mass of water (w) related mass of cement (s) + mass of fibers (f).

θ and δ are concentrations directly calculated from the mass m of each component (of known density ρ)

4. Results and discussion

In order to estimate thermal conductivity of vegetable fibers, some properties of composites are required: physical properties (bulk dry density, open porosity) and thermal conductivity.

4.1 Bulk density and open porosity of composites at 0% RH

Figure 4 reports the variation of bulk density as a function of the fiber contents for LFN composites in the dry state. As expected, the more the fiber content, the lower the bulk density is [36]. The first significant decrease is obvious: it corresponds to the addition of 2% by weight of bagasse fibers, which are a lightweight material. Between 2 and 4% by weight of fibers, there is a light decrease. After 4 wt%, bulk density decreased at a relatively constant rate with increased fiber content as observed by [37].

Figure 5 presents the evolution of LFN composites porosity according to their fiber content in the dry state.

Porosity of material is gradually increasing with the amount of bagasse fibers. This increase with addition of fibers is explained by the formation of air voids in the microstructure of paste (due to the presence of fibers which are porous) and the voids content becomes high as fiber volume fraction increases [36]. Moreover, short fibers, as used in this study, are considered to be more difficult to align and pack densely. The

packing of short fibers in cement paste leads to increase the amount of voids [10] and therefore porosity.

4.2 Thermal conductivity of composites

4.2.1 Experimental thermal conductivity

4.2.1.1 Dry state

Figure 6 illustrates the evolution of thermal conductivity of LFN composites according to fiber content at 0% of relative humidity. According to Demirboga [38], thermal conductivity of Portland cement type I is (1.230 +/- 0.050) W/m.K.

The purpose of including vegetable fibers in cement is to develop a more insulating material than cement in order to use it as an interior partition or an interior insulating coating in the housing, for examples. It would help to prohibit the leaking of heat on both sides of the partitions [36]. First, as expected, the thermal conductivity of Portland cement is strongly decreased (by a factor of around 2) by introducing 2 wt % of vegetable fibers. Then, thermal conductivity of cement samples decreases slightly when increasing fiber content [10, 27, 36]. This decrease follows a logarithmic evolution. According to [3], thermal conductivity of treated bagasse fibers is lower than that of cement paste, so we assume it's the same for raw bagasse fibers: its thermal conductivity is lower than that of cement. Consequently, this decrease is expected with law of mixture. Moreover, thermal conductivity is inversely proportional to the voids in composites [10, 39] and as shown by Figure 5, porosity of samples increases with the fiber content. Based on these results, the linear relation between the thermal conductivity k of bagasse composites and bulk density ρ is:

$$k = 0.0005\rho - 0.0924 \left(R^2 = 0.78267\right) \qquad \text{equation 6}$$

where k is thermal conductivity and ρ bulk density.
Equation 6 is consistent with classical equations applied to evaluate thermal conductivity of insulating materials used in the field of construction [39].

4.2.1.2 Sensitivity of thermal conductivity to moisture content

Thermal conductivity was also studied for the same composites at 56% and 100% of relative humidity (saturated state).
Fibrous media are known to often have a geometric anisotropy linked (1) to the anisotropy of the fibers themselves and (2) to their orientation within the material. In the case of vegetable fibers, an anisotropy of the thermal properties appears locally, as the tensor of conductivity of fibers is generally orthotropic [38]. We assume that the thermal conductivity of studied composites is isotropic because fibers are randomly oriented and properties of short fibers (in this study, length varying from 1 to 10 mm and width between 0.4 and 1 mm) composites are isotropic [41].
Figure 7 presents the thermal conductivity of samples according to their bulk density for different moisture contents.
The more the percentage of pores, the lighter the specimen are and the lower their thermal conductivities are as observed by others [10]. That is to say that the lighter a material is and the better is its insulating power. The thermal conductivity of the composites in saturated conditions is greater than in the dry state [27]. This fact is explained by the thermal conductivity of water, which is 25 times higher than air [42];

the presence of air will alter the overall thermal conductivity of the material by decreasing it. The composite subjected to a relative humidity of 56% exhibited a mass gain of 4 to 8% (in comparison with dry state), which involves the increase from 15 to 50% of the thermal conductivity of materials. For moisture contents close to saturation, the thermal conductivity of the composite increases by around 100 % of its value in the dry state. These results are in accordance with those exhibited by Asadi et al. [39].

4.2.2 Numerical thermal conductivity

4.2.2.1 Dry state

Firstly, by knowing the thermal conductivity of pure hardened cement paste, λ_d and its porosity measured with helium pycnometer, we can calculate the conductivity of solid particles λ_s using equation 2. The value of λ_s is 1.125 W/m.K.
To estimate thermal conductivity of fibers, the auto-coherent method applied to three phases medium (equation 3) is used in combination with least squares method of minimization. The mean square deviation between experimental and numerical thermal conductivities of dry composites is minimized and bagasse fibers thermal conductivity is estimated. Its average value is about 0.110 W/m.K. This value is consistent with the values estimated by Onésippe et al. [3] for treated bagasse fibers.

Figure 8 shows that the theoretical values calculated using equation 3 are consistent with the experimental measurements in the case of dry composites, whatever the bulk density. A gap of less than 10% is obtained.

4.2.2.2. Wet state (100% RH)

As with the previous model, a comparison of the results is made in the case of wet composites (56% RH, Figure 9 and 100% RH, Figure 10). For 56% RH, there is a good agreement between numerical and experimental values in low fibers contents (approx. less than 4 wt%), which correspond to bulk densities greater than 1360 kg/m^3. Below this value, it seems that the model underestimates thermal conductivity of composites by about 10 to 20%. This underestimation reaches nearly 30% at saturated state (100% RH), whatever the bulk density, as shown by Figure 10. The model used for numerical calculation considered the shape of the aggregates to be spherical. This underestimation may be due to the geometrical distribution of void phase that is to say distribution of pore structure. This difference can also be explained by conduction phenomenon due to free water or entrapped water that implies the use of a more complex modeling to explain the behavior. Moreover, the experimental conductivity is the average of local measurements that depend on surface conditions, orientation of fibers and compacting direction. In addition, polishing of samples with high fiber content is difficult and can cause local differences in thickness.
The thermal conductivity calculated by the model seems to be little sensitive to changes induced by the generic water cell. This little sensitivity is explained by low volume of water adsorbed in this range of humidity.

5. Perspectives

Generally, in Guadeloupe, the relative humidity of the air varies between 70% and 80% [42], that is to say that the thermal conductivity of composites would be greater than in the dry state. The composites of this study cannot be considered as insulating materials for our climatic conditions. In order to decrease their thermal conductivity, we

considered treatment of bagasse fibers before incorporating them into Portland cement. We choose to analyze the effect of pyrolysis treatment on sorption/desorption behaviors of the bagasse fibers. The sorption isotherm of natural bagasse fibers NBF is compared to that of pyrolyzed fibers, TBF which are prepared under controlled inert atmosphere (N_2 flow, 2 L/h) during 2 h at 240°C [43]. It is obtained experimentally by assessing the moisture content of the product in equilibrium with different air relative humidity at an average temperature of (22±3) °C. Relative humidity is controlled by saturated saline solutions according to ISO-12571 norm [44]. The moisture content *w* is deduced using the equation 7:

$$w = \frac{m - m_0}{m_0} \qquad \text{equation 7}$$

Where *m* and m_0 are the mass of the sample in respectively steady state conditions and initial dry state.

In Figure 11, the isotherms present a S-shape corresponding to the type IV of the Rogers classification. This behavior is frequently observed in cellulose-based materials [45]. We can see that pyrolyzed bagasse fibers are less hygroscopic than natural bagasse fibers, particularly at high relative humidity (decrease of 30% of its sorption capacity). Indeed, hemicellulose degradation during pyrolysis (between 160 and 260°C) [32] makes the TBF less sensitive to moisture; generally, they become more hydrophobic [3]. This last point encourages us to develop pyrolyzed bagasse fiber / cement composites. As mentioned by Collet and Pretot [28], thermal conductivity of hygroscopic materials increases with moisture content. The pyrolyzed fibers being more hydrophobic [3] than the raw fibers, they would generate less moisture in the composites that is to say that the ratio air/water will be increased. As thermal conductivity of air is lower than that of water [35], the resulting composites would have lower thermal conductivities (if we consider a simple law of mixture) than the LFN and would allow our materials to be considered as insulating materials in the field of construction.

6. Conclusions

A theoretical modeling based on auto-coherent homogenization is proposed to estimate the thermal conductivity of bagasse fibers, that is a novelty. The model is also used to estimate the conductivity of fibers and cement and then the conductivity of composites under both dry (good fitting with the model) and wet conditions.

The bagasse fibers / cement composites materials present low thermal conductivity. The study shows that the thermal conductivity of such composites depends both on fibers / cement ratio (bulk density) and moisture content. The best insulating properties are obtained with an untreated bagasse fiber content around 8 % wt.

Further investigations on pores size and distribution are required in order to improve the accuracy of the model in wet conditions.

We explore the isotherm sorption of pyrolyzed bagasse fibers. These data confirm that the pyrolysis allows obtaining more hydrophobic fibers, which once included in cement, would provide more insulating materials for building applications.

Acknowledgements

We thank for the financial support (1) the Région Guadeloupe and european funds for projects “Développement d’isolants thermiques à partir de fibres végétales : ISOCFV” (n°32524) and (2) the Agence Nationale de la Recherche for the project

"AWaPUMat/Résidus industriels, leurs usages potentiels comme matériaux pour l'habitation et la construction" (n° ANR-12-IS09-0002-01).

References

[1] M.A. Arsène, K. Bilba, C. Onésippe, L. Rodier, Thermal and flexural properties of bagasse/cement composites, J. Green Mater. (2016). http://dx.doi.org/10.1680/jgrma.1500012

[2] R.C. Dromard, Y. Bouchon-Navaro, S. Cordonnier, C. Bouchon, The invasive lionfish, Pterois volitans, used as a sentinel species to assess the organochlorine pollution by chlordecone in Guadeloupe (Lesser Antilles), J. Mar. Pol. Bul. 107 (2016) 102-106. https://doi.org/10.1016/j.marpolbul.2016.04.012

[3] C. Onésippe, N. Passé-Coutrin, F. Toro, S. Delvasto, K. Bilba, M.A. Arsène, Sugar cane bagasse fibres reinforced cement composites : Thermal considerations, J. Compos. Part A Appl. Sci. Manuf. 41 (2010) 549-556. https://doi.org/10.1016/j.compositesa.2010.01.002

[4] J. Faverial, J. Sierra, Home composting of household biodegradable wastes under the tropical conditions of Guadeloupe (French Antilles), J. Cleaner Prod. 83 (2014) 238-244. https://doi.org/10.1016/j.clepro.2014.07.068

[5] N. Zahibo, E. Pelinovsky, T. Talipova, A. Rabinovich, A. Kurkin, I. Nikolkina, Statistical analysis of cyclone hazard for Guadeloupe, Lesser Antilles, Atmosph. Res. 84 (2007) 13-29. https://doi.org/10.1016/j.atmosres.2006.03.008

[6] L. Rodier, Matériaux de construction en zone tropicale humide - Potentialités de sous produits ou de matériaux naturels locaux en substitution ou en addition à la matrice cimentaire, Doctoral thesis (2014), Université des Antilles et de la Guyane (France)

[7] L. Rodier, K. Bilba, C. Onésippe, M.A. Arsène, Utilization of bio-chars from sugarcane bagasse pyrolysis in cement-based composites, J. Ind. Crop 41 (2019) 111731. https://doi.org/10.1016/j.indcrop.2019.111731

[8] J.C. Damfeu, P. Meukam, Y. Jannot, Modeling and measuring of the thermal properties of insulating vegetable fibers by the asymmetrical hot plate method and the radial flux method : Kapok, coconut, groundnut shell fiber and rattan, J. Thermochimica Acta 630 (2016) 64-77. https://doi.org/10.1016/j.tca.2016.02.007

[9] V. Agopyan, H. Savastano Jr., V. M. John, M. A. Cincotto, Developments on vegetable fibre-cement based materials in Sao Paulo, Brazil : an overview, J. Cem. Concr. Compos. 27 (2005) 527-536. https://doi.org/10.1016/j.cemconcomp.2004.09.004

[10] J. Khedari, B. Suttisonk, N. Prathinthong, J. Hirunlabh, New lightweight composite construction materials with low thermal conductivity, J. Cem. Concr. Comp. 23 (2001) 65-70. https://doi.org/S0958-9465(00)00072-X.

[11] V. Da Costa Correia, S.F. Santos, H. Savastano Junior, Vegetable fiber as reinforcing elements for cement based composite in housing applications – a Brazilian experience, MATEC Web Conf. 149 (2018) 01007. https://doi.org/10.1051/matecconf/201814001007

[12] M.-A. Arsène, K. Bilba, C. Onésippe, 4- Treatments to viable utilization of vegetable fibers in inorganic-based composites, in : H. Savastano Junior, J. Fiorelli, S. F. dos Santos (Eds.), Sustainable and nonconventional contruction materials using inorganic bonded fiber composites, Woodhead publishing Inc., Sao Paulo, 2017, pp. 69-123

[13] F. Collet, Caractérisations hydrique et thermique de matériaux de génie civil à faibles impacts environnementaux, Doctoral thesis (2004), INSA de Rennes (France)
[14] S.F. Santos, G.H.D. Tonoli, J.E.B. Mejia, J. Fiorelli, H. Savastano Junior, Non-conventional cement-based composites,reinforced with vegetable fibers: A review of strategies to improve durability, Materiales de Construccion 65 (2015) e041. https://doi.org/10.3989/mc.2015.05514.
[15] V. Cerezo, Propriétés mécaniques, thermiques et acoustiques d'un matériau à base de particules végétales, Doctoral thesis (2005), INSA de Rennes (France)
[16] P. Coatanlem, R. Jauberthie, F. Rendell, Lightweight wood chipping concrete durability, J. Constr. Build. Mater. 20 (2006) 776-781. https://doi.org/10.1016/j.conbuildmat.2005.01.057
[17] T.T. Nguyen, V. Picandet, S. Amziane, C. Baley, Influence of compactness and hemp hurd characteristics on the mechanical properties of lime and hemp concrete, European journal of environmental and civil engineering 13 (2009) 1039-1050. https://doi.org/ 10.3166/regc.13.1039-1050
[18] P. Monreal, L.B. Mboumba-Mamboundou, R.M. Dheilly, M. Queneudec, Effects of aggregate coating on the hygral properties of lignocellulosic composites, J. Cem. Concr. Compos. 33 (2011) 301-308. https://doi.org/10.1016/j.cemconcomp.2010.10.017
[19] J. Page, F. Khadraoui, M. Gomina, M. Boutouil, Influence of different surface treatments onthe water absorption of flax fibres : rheology of fresh reinforced-mortars and mechanical properties in the hardened state, Constr. Build. Mater. 199 (2019) 424-434. https:// oi.org/10.1016/j.conbuildmat.2018.12.042
[20] Direction de l'Alimentation, de l'Agriculture et de la Forêt de Guadeloupe. http://daaf.guadeloupe.agriculture.gouv.fr/Canne-a-sucre, 2019 (accessed 09 april 2019)
[21] S.G. Karp, A. Lorenci Woiciechowski, V.T. Soccol, C. R. Soccol, Pretreatment strategies for delignification of sugarcane bagasse: a Review, Braz. Arch. Biol. Technol. 56 (2013) 679-689.
[22] M.I. Khan, Factors affecting the thermal properties of concrete and applicability of its prediction models, J. Build. and Environ. 37 (6) (2002) 607-614. https://doi.org/10.1016/S0360-1323(01)00061-0
[23] J. Wang, J.K. Carson, M.F. North, D.J. Cleland, A new structural model of effective thermal conductivity for heterogeneous materiald with co-continuous phases, International J. Heat Mass Transfer 21 (9-10) (2008) 2389-2397. https://doi.org/10.1016/j.ijheatmasstransfer.2007.08.028
[24] P.K. Samantray, P. Karthikeyan, K.S. Reddy, Estimating effective thermal conductivity of two-phase materials, J. Heat Mass Transfer 49 (21-22) (2006) 4209-4219. https://doi.org/10.1016/j.ijheatmasstransfer.2006.03.015
[25] M. Bederina, L. Marmoret, K. Mezreb, M.M. Khenfer, A. Bali, M. Quéneudec, Effect of addition of wood shavings on the thermal conductivity of sand concretes : experimental study and modelling, J. Constr. Build. Mater. 21 (2007) 662-668. https://doi.org/10.1016/j.conbuildmat.2005.12.008
[26] A. Benazzouk, O. Douzane, K. Mezreb, B. Laidoudi, M. Quéneudec, Thermal conductivity of cement composites containing rubber waste particles : experimental study and modelling, J. Constr. Build. Mater. 22 (2008) 573-579. https://doi.org/10.1016/j.conbuildmat.2006.11.011
[27] L. Boukhattem, M. Boumhaout, H. Hamdi, B. Benhamou, F. Ait Nouh, Moisture content influence on the thermal conductivity of insulating building materials made

525 from date palm fibers mesh, J. Constr. Build. Mater. 148 (2017) 811-823.
526 https://doi.org/10.1016/j.conbuildmat.2017.05.020
527 [28] F. Collet, S. Pretot, Thermal conductivity of hemp concretes: Variation with
528 formulation, density and water content, J. Constr. Build. Mater. 65 (2014) 612-619
529 https://doi.org/10.1016/j.conbuidmat.2014.05.039
530 [29] C. Boutin, Thermal conductivity of autoclaved aerated concrete: modeling by the
531 self-consistent method, J. Mater. Struct. 29 (1996) 609-615
532 https://doi.org/10.1007/BF02485968
533 [30] J.D. Felske, Effective thermal conductivity of composite spheres in a continuous
534 medium with contact resistance, Int. J. Heat Mass Transf. 47 (2004) 3453-3461
535 https://doi.org/j.ijheatmasstransfer.2004.01.013
536 [31] G. Ruano, F. Bellomo, G. Lopez, A. Bertuzzi, L. Nalim, S. Oller, Mechanical behavior of
537 cementitious composites reinforced with bagasse and hemp fibers, J. Construct. Build.
538 Mater. 240 (2020) 117856
539 https://doi.org/10.1016/jconbuidmat.2019.117856
540 [32] K. Bilba, M.-A. Arsène, A. Ouensanga, Sugar cane bagasse reinforced cement
541 composites. Part I. Influence of the botanical components of bagasse on the setting of
542 bagasse/cement composite, J. Cem. Concr. Compos. 25 (2003) 91–96.
543 https://doi.org/10.1016/S0958-9465(02)00003-3
544 [33] EN 197-1, Ciment – Partie 1 : composition, spécifications et critères de conformité
545 des ciments courants, NF European Standards, 2001
546 [34] EN 196-1, Méthodes d'essais des ciments – Partie 1 : détermination des résistances
547 mécaniques, NF European Standards, 2006
548 [35] SETARAM. https://www.setaram.fr/wp-content/uploads/2016/01/C-Therm-TCi-
549 Thermal-Conductivity-2016.pdf, 2019 (accessed 11 april 2019)
550 [36] A. Al-Ghaban, H.A. Jaber, A.A. Shaher, Investigation of addition different fibers on
551 the performance of cement mortar, J. Eng. Tech. Part A 36 (2018) 957-965.
552 http://dx.doi.org/10.30684/etj.36.9A.3
553 [37] H. Savastano Jr., P.G. Warden, R.S.P. Coutts, Brazilian waste fibres as reinforcement
554 for cement-based composites, J. Cem. Concr. Compos. 22 (2000) 379-384.
555 https://doi.org/10.1016/S0958-9465(00)00034-2
556 [38] R. Demirboga, Thermal conductivity and compressive strength of concrete
557 incorporation with mineral admixtures, J. Build. Env. 42 (2007) 2467-2471.
558 http://dx.doi.org/10.1016/J;buidenv.2006.06.010
559 [39] I. Asadi, P. Shafigh, Z. Fitri Abu Hassan, N. Bindi Mahyuddin, Thermal conductivity of
560 concrete – a review, J. Build. Eng. 20 (2018) 81-93.
561 https://doi.org/10.1016/j.jobe.2018.07.002
562 [40] R. El-Sawalhy, J. Lux, P. Salagnac, Caractérisation et prédiction des propriétés
563 thermiques des laines de chanvre à l'aide d'images tomographiques, Conference paper
564 (2013)
565 [41] Gaurav, H. Gohal, V. Kumar, H. Jena, Study of natural fibre composite and its
566 hybridization techniques, J. Mater. Today: Proceedings (2020) *In press*
567 https://doi.org/10.1016/j.matpro.2020.02.277
568 [42] Weather online, 2019 (accessed 11 april 2019)
569 https://www.wofrance.fr/weather/maps/city?WMO=78897&CONT=mamk&LAND=AT
570 &ART=RLF&LEVEL=150
571 [43] K. Bilba, M.-A. Arsène, Silane treatment of bagasse fiber for reinforcement of
572 cementitious composites, J. Compos. Part A Appl. Sci. Manuf. 39 (2008) 1488-1495.
573 https://doi.org/10.1016/j.compositesa.2008.05.013

[44] ISO-12571 Performance hygrothermique des matériaux et produits pour le bâtiment – Détermination des propriétés de sorption hygroscopiques, International Organization for Standardization, 2013
[45] A. Bessadok, D. Langevin, F. Gouanvé, C. Chappey S. Roudesli, S. Marais, Study of water sorption on modified agave fibres, Carbohydr. Polym. 76 (2009) 74-85. https://doi.org/10.1016/j.carbpol.2008.09.033

Figures caption

Figure 1 : Auto-coherent method applied to two-phase medium - geometry of an elementary inclusion composite
Where R_a and thermal conductivity λ_a (component "a" is the air contained within the vegetable fibers) surrounded by a concentric shell of component "s" (s is the fiber block) of thermal conductivity λ_s and radius R_s, λ_d is the thermal conductivity of the equivalent homogeneous material also called effective conductivity

Figure 2 : Auto-coherent method applied to three-phase medium - geometry of an elementary inclusion composite
Where a spherical air bubble "a" is surrounded by a concentric vegetable particles shell "f " itself surrounded by a binder shell "s"

Figure 3 : Double homogenization of auto-coherent model (binder+ vegetable particles)
Where a is for air, w is for water and H for hydrated composite

Figure 4 : Bulk density of composites according to their fiber content in the dry state (RH = 0%)

Figure 5 : Porosity of composites according to their fiber content in the dry state (RH = 0%)

Figure 6 : Experimental thermal conductivity of LFN composites according to their fiber content in the dry state (RH = 0%)

Figure 7 : Experimental thermal conductivity of LFN composites according to their bulk density at different moisture contents

Figure 8 : Comparison between numerical calculations and experimental results of composites thermal conductivity in the dry state according to bulk density

Figure 9 : Thermal conductivity varying with bulk density: comparison between numerical calculations and experimental results in the wet state (RH=56%)

Figure 10: Thermal conductivity varying with bulk density: comparison between numerical calculations and experimental results in the wet state (RH=100%)

Figure 11 : Isotherm sorption of natural (NBF) and pyrolyzed bagasse fibers (TBF) at (22±3)°C. In red: sorption; in green: desorption.

Table 1: Botanical composition of raw sugar cane bagasse fibers (NBF) [29].

Cellulose	Hemicellulose	Lignin	Extractives	Humidity	Sum (except humidity)
wt %	wt %	wt %	wt %	wt %	wt %
48.68	25.46	21.94	3.92	7.50	100

Table 2: Chemical composition and some physical characteristics of CEM I 52,5 N [5].

Content wt %						
SiO_2	Fe_2O_3	Al_2O_3	CaO	Na_2O	K_2O	MgO
21.45	0.22	4.08	65.05	0.06	0.20	0.49
Loss on ignition (wt %)						
1.45						
Bulk density (g/cm³)						
3.08						
Median particle size (µm)						
15.70						
Specific area (cm²/g)						
4200						

Table 3 : Formulations of LFN composites.

Composites	Binder	NBF/binder ratio (by mass)	Water/binder ratio (by mass)	Mass (g) relative to 1000 g of cement paste		
				NBF	CEM I	Water
L (without fibers)	1	0	0.4	0	704	296
LFN1	1	0.02	0.60	12.3	617.3	370.4
LFN2	1	0.03	0.60	18.4	613.5	368.1
LFN3	1	0.04	0.60	24.4	609.8	365.8
LFN4	1	0.05	0.60	30.3	606.1	363.6
LFN5	1	0.08	0.60	47.6	595.2	357.2

Table 4 : Mixing sequence of elaboration of composites.

Mixing sequence	Time
Adding the pre-wetted binder in the mixing container	0
Mixing the binder at slow speed (140 rpm)	30 s
Adding the rest of the water	30 s
Mixing at high speed (285 rpm)	2 min
Progressive addition of vegetable fibers	2 min
Mixing at high speed (285 rpm)	5 min

Figure 1 : Auto-coherent method applied to two-phase medium - geometry of an elementary inclusion composite

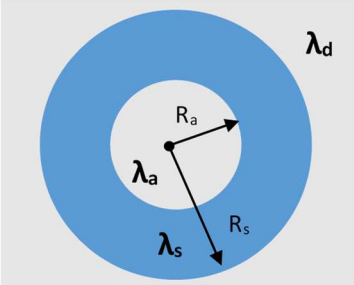

Figure 2 : Auto-coherent method applied to three-phase medium - geometry of an elementary inclusion composite

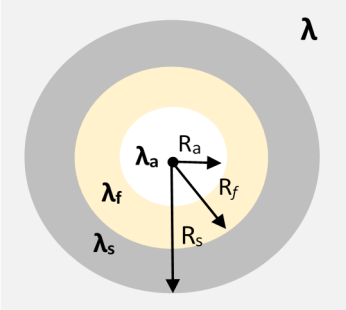

Figure 3 : Double homogenization of auto-coherent model (binder+ vegetable particles) where a is for air, w is for water and H for hydrated composite

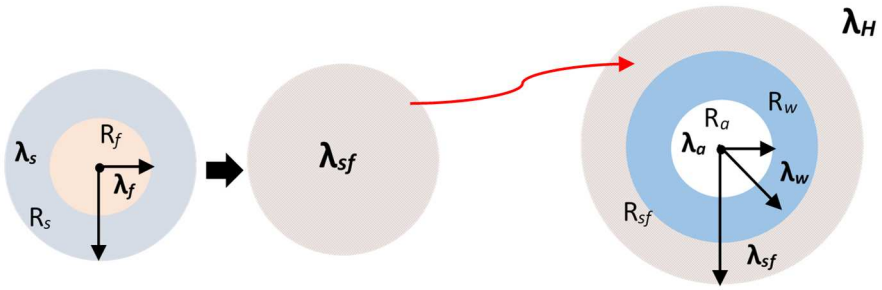

Figure 4 : Bulk density of composites according fiber content in the dry state (RH = 0%)

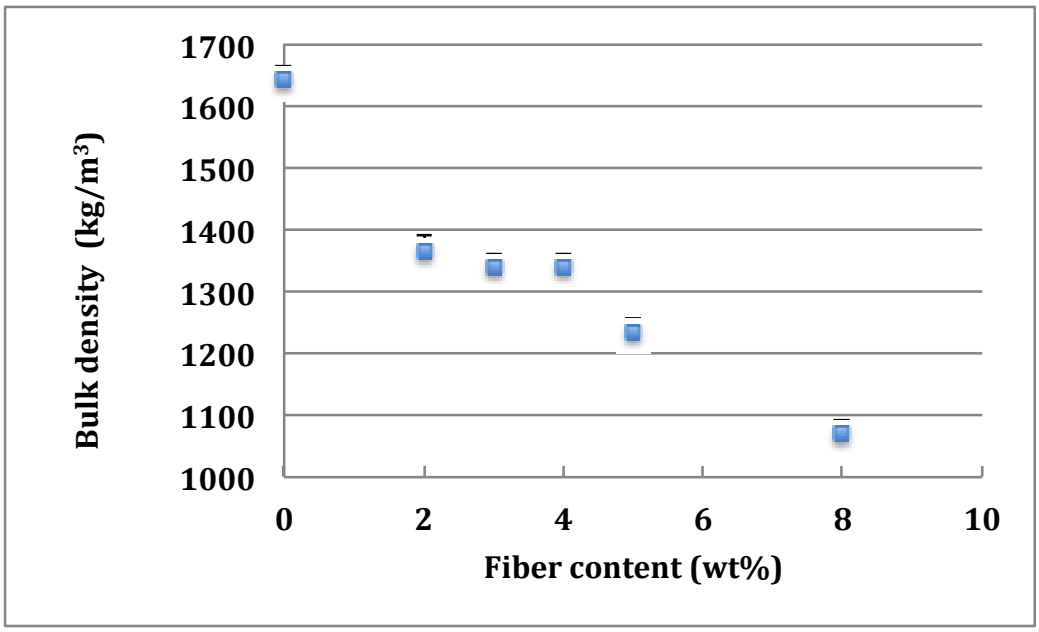

Figure 5 : Porosity of composites according to their fiber content in the dry state (RH = 0%)

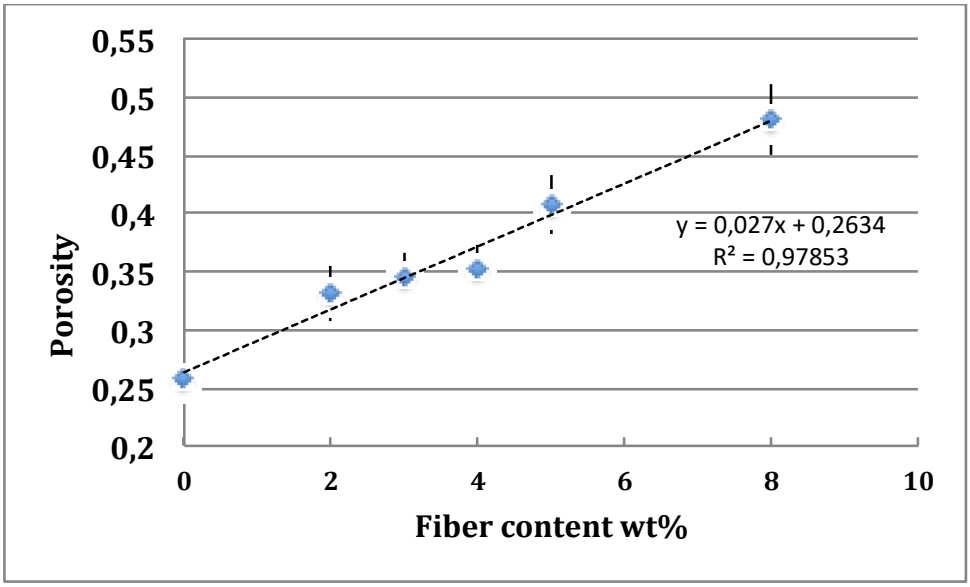

Figure 6 : Thermal conductivity of LFN composites according to fiber content

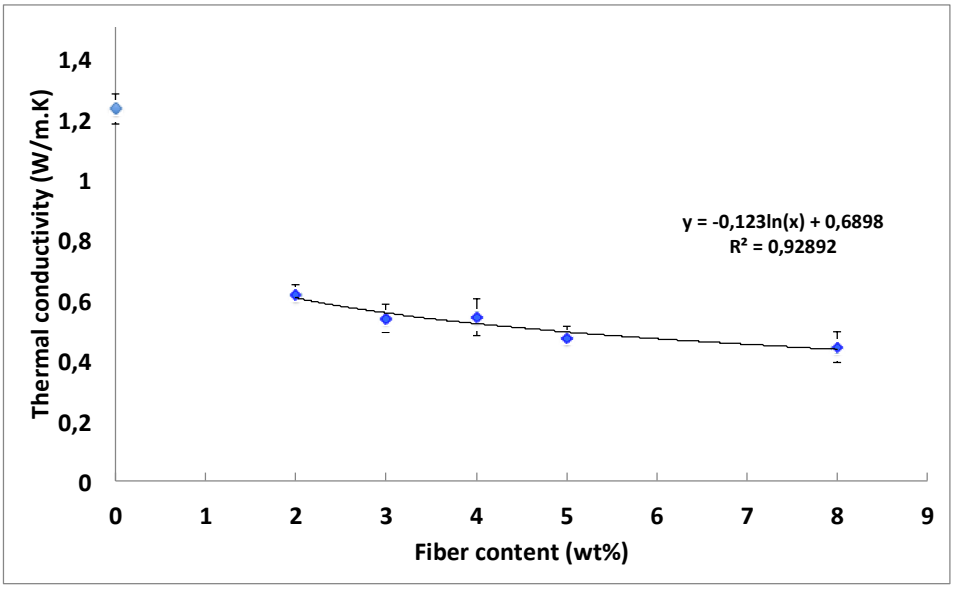

Figure 7: Thermal conductivity of LFN composites according to their bulk density at different moisture contents

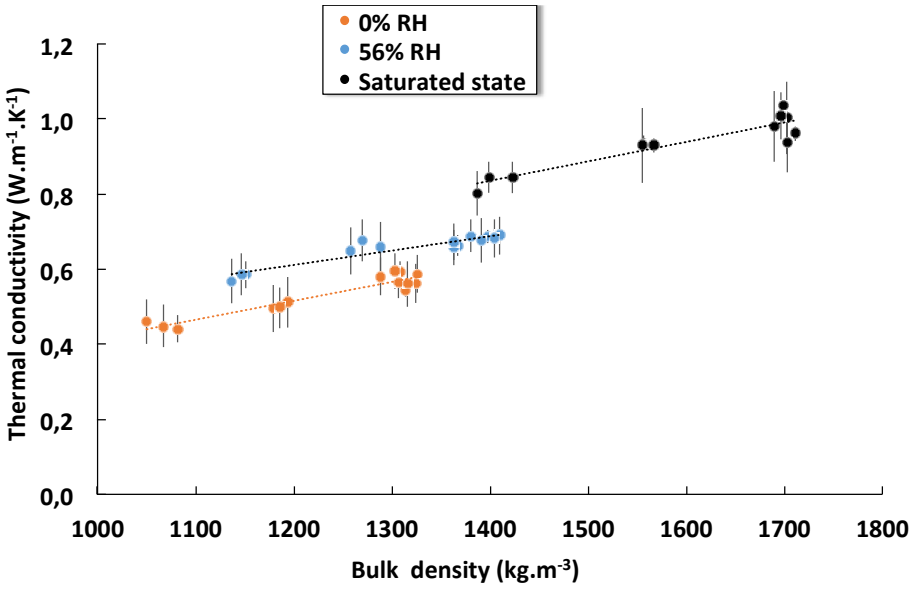

Figure 8: Comparison between theoretical calculations and experimental results of thermal conductivity of dry composites according to bulk density

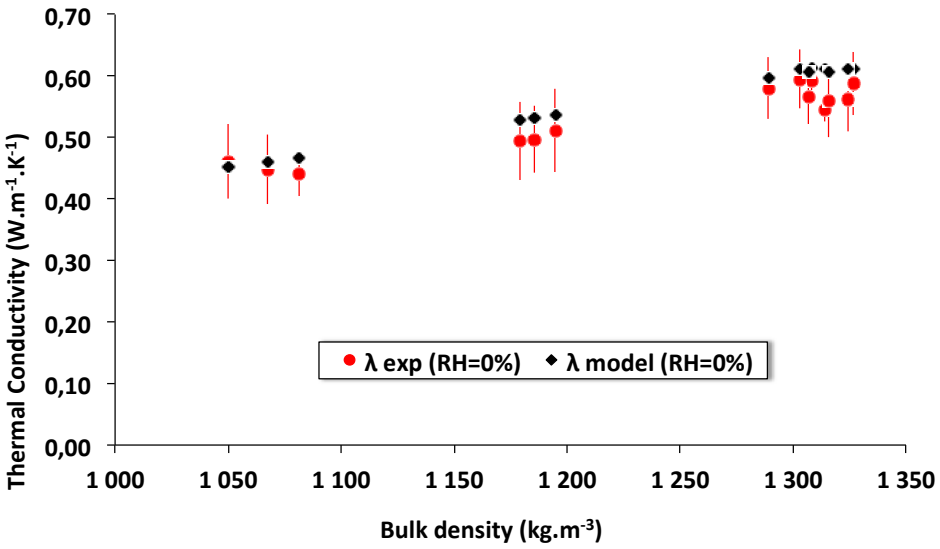

Figure 9: Thermal conductivity varying with bulk density: comparison between theoretical calculations and experimental results (RH=56%)

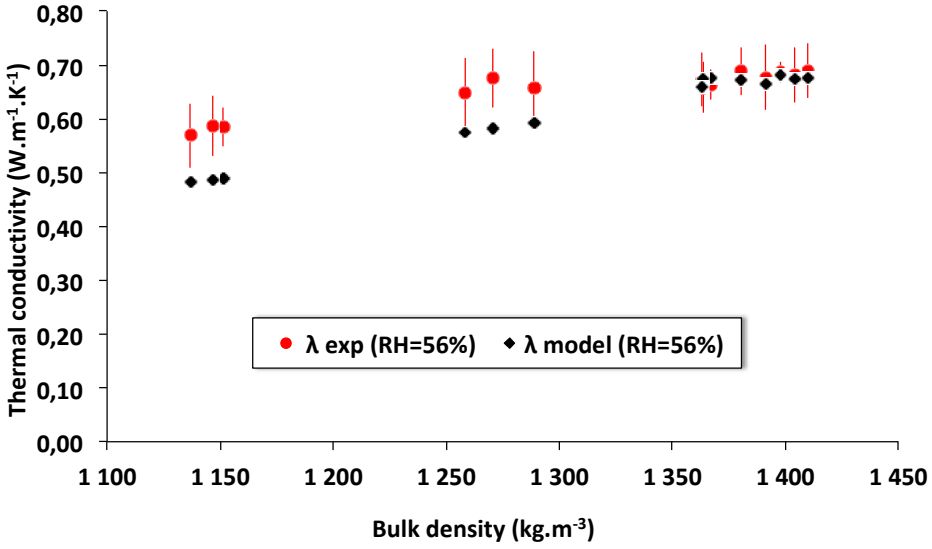

Figure 10: Thermal conductivity varying with bulk density: comparison between theoretical calculations and experimental results (RH=100%)

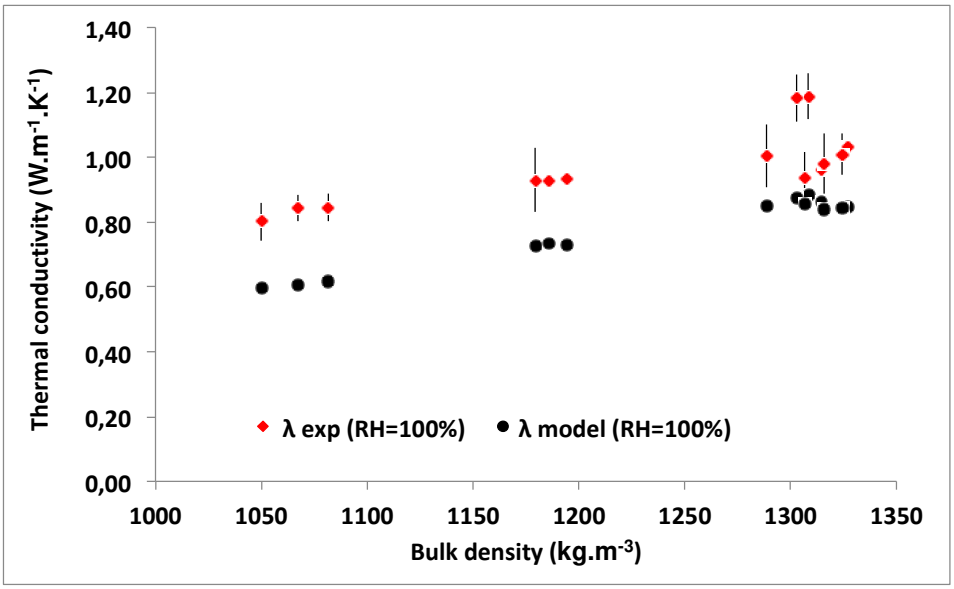

Figure 11 : Sorption isotherms of natural (NBF) and pyrolyzed (TBF) bagasse fibers at (22±3)°C. In red: sorption; in green: desorption.